BIOCHEMISTRY
including biophysical chemistry & molecular biology
Rapid Report

Biochemistry **2010,** *49,* 9425–9427 9425
DOI: 10.1021/bi101502v

Conformational Changes in the G Protein-Coupled Receptor Rhodopsin Revealed by Histidine Hydrogen−Deuterium Exchange†

David T. Lodowski,*,‡ Krzysztof Palczewski,*,‡ and Masaru Miyagi*,‡,§

‡*Department of Pharmacology, Case Western Reserve University, School of Medicine, Cleveland, Ohio 44106-4965, United States, and* §*Center for Proteomics and Bioinformatics, Case Western Reserve University, Cleveland, Ohio 44106-4965, United States*

Received September 15, 2010; Revised Manuscript Received October 11, 2010

ABSTRACT: G protein-coupled receptors (GPCRs) are activated by ligand binding, allowing extracellular signals to be efficiently transmitted through the membrane to the G protein recognition site, 40 Å away. Utilizing His residues found spaced throughout the GPCR, rhodopsin, we used His hydrogen−deuterium exchange (His-HDX) to monitor long-time scale structural rearrangements previously inaccessible by other means. The half-lives of His-HDX indicate clear differences in the solvent accessibility of three His residues in rhodopsin/opsin and Zn^{2+}-dependent changes in the pK_a for His^{195}. These results indicate the utility of His-HDX in examining structural rearrangements in native source and membrane proteins without requiring structural modification.

Rhodopsin (Rho), the G protein-coupled receptor (GPCR) in the eye responsible for dim light vision, was the first GPCR to have its atomic structure determined and now serves as a prototypical GPCR for the purpose of understanding G protein signaling (*1*). Rho is composed of the apoprotein, opsin, and a covalently coupled 11-*cis*-retinal chromophore. Upon light exposure, isomerization of the chromophore to its all-*trans* state drives Rho through a series of photointermediates that culminate in its active signaling state, Meta II. After attainment of Meta II, the chromophore is hydrolyzed to form the inactive apoprotein, opsin, and free all-*trans*-retinal.

The process by which an extracellular activation signal of the GPCR is passed through the cell membrane to the recognition site of cytoplasmic interacting proteins has not been fully elucidated (*2*). For Rho (*1*), X-ray crystallographic structures of Rho photointermediates and opsin show only minor changes in the receptor helical bundle (*3*, *4*) upon photoactivation, in stark contrast to early studies that predicted large scale rigid body motions on the order of 20 Å (*5*). This observation poses the question of what the mechanism by which this signal is transmitted through the transmembrane domain of GPCRs is. Studies of the seven-transmembrane spanning but unrelated protein, bacteriorhodopsin, indicated an essential role for internal waters in light-induced proton transfer by this protein (*6*).

Recently, we used X-ray radiation-induced hydroxyl radical labeling in tandem with mass spectroscopy to probe dynamic changes of ordered waters within the transmembrane region of Rho upon photoactivation (*7*). Whereas this method is exquisitely sensitive for observing millisecond time scale changes in conformation and flexibility within the transmembrane region upon photoactivation, it cannot directly measure changes in solvent exposure or protonation state. While recent amide hydrogen−deuterium exchange (HDX) studies have successfully provided data about solvent accessibility and ligand-dependent conformational changes in the membrane proteins γ-glutamyl carboxylase and β_2-adrenergic receptor (*8*, *9*), respectively, amide HDX is not suitable for accurately capturing longer time scale changes in water accessibility to the core of the receptor.

His residues have been postulated to play important roles in the Meta I−Meta II equilibrium and activation process of Rho (*10*, *11*). These residues are distributed throughout the three-dimensional structure (Figure 1A), and located in critical regions of the protein involved in dimerization and/or oligomerization (Figure 1B), and serve as components of its physiologically relevant, divalent ion binding sites (Figure 1D). Specific environments of each His residue in Rho are depicted in Figure S-1 of the Supporting Information. In an effort to extend these observations, we employed a novel mass spectrometry-based method to visualize changes in the solvent accessibility of Rho, relying on the specific, slow exchange of the C_2 hydrogen of the imidazole ring in His residues with deuterium (*12*) (Figure 2A−C), rather than the more general amide HDX which is a convolution of solvent accessibility, short-time scale protein dynamics, and intrinsic amide H exchange rates.

Thus, we used these His residues as intrinsic probes to monitor structural changes during Rho activation, eliminating artifacts due to protein modification. Also, the apparent pK_a values of His^{195} residues within the protein were calculated by coupling this exchange to a pH titration; the pK_a values of one of the His residues (His^{195}) in different structural states were determined (Figure 2D). By computing changes in the rate of exchange for individual His residues, we calculated the half-life ($t_{1/2}$) of HDX, which inversely relates to the His residue's solvent accessibility. Table 1 shows the half-lives of HDX obtained for all His residues in the Rho native membrane. We also determined the pK_a for His^{195} that varied depending on ionic conditions because of the known allosteric regulator Zn^{2+} and the presence or absence of lipids (Figure 2D).

In Rho and opsin, transmembrane His^{152} and His^{211} did not undergo HDX, most likely because D_2O cannot penetrate the membrane and exchange with internal ordered (H_2O) waters within the transmembrane segment of these proteins. These results are consistent with footprinting data (*7*). His^{278} also did not

†This research was supported in part by Grants EY008061 and EY019718 and Core Grant P30 EY011373 from the National Institutes of Health.

*To whom correspondence should be addressed. D.T.L.: e-mail, dtl10@case.edu; phone, (216) 368-8794; fax, (216) 368-1300. K.P.: e-mail, kxp65@case.edu; phone, (216) 368-4497; fax, (216) 368-1300. M.M.: e-mail, mxm356@case.edu; phone, (216) 368-5917; fax, (216) 368-6846.

Published on Web 10/12/2010

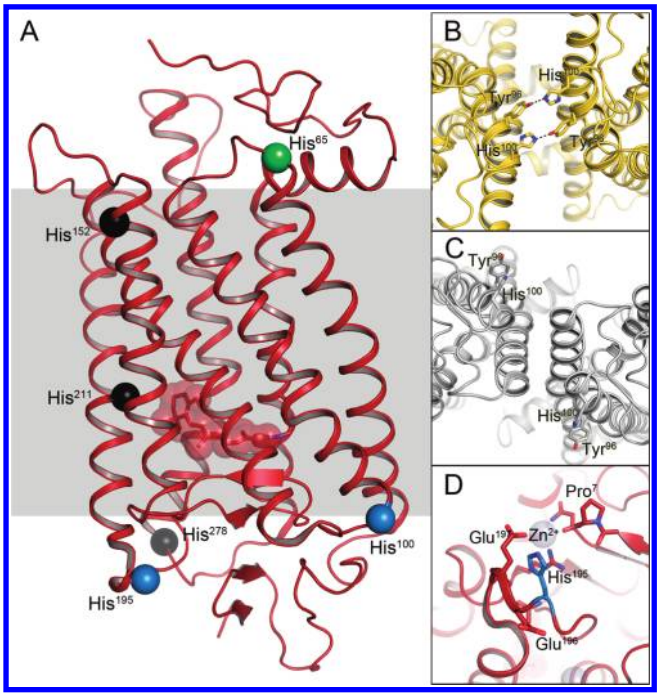

FIGURE 1: Positions of His residues in the Rho structure. (A) The Cα positions of each of the six His residues in bovine Rho are represented as colored spheres: black spheres for His^{152}, His^{211}, and His^{278} with a half-life of deuterium exchange greater than 50 days, blue spheres for His^{100} and His^{195}, which exchange more slowly in opsin than Rho, a green sphere for His^{65}, which exchanges more rapidly in opsin than Rho, and a transparent red spheres for the 11-*cis*-retinylidiene chromophore. (B and C) Crystallographically observed dimers may explain the differential in deuterium exchange. In photoactivated Rho [Protein Data Bank (PDB) entry 2I37], His^{100} has an interaction with Tyr^{96} not observed in the opsin structure (PDB entry 3CAP). (D) A bound Zn^{2+} ion is observed in tetragonal Rho structures (e.g., PDB entries 1F88 and 1U19) that interact directly with His^{195}. This interaction may be both physiologically important for stabilizing Rho and explain the Zn^{2+}-dependent shifts in the pK_a of this residue.

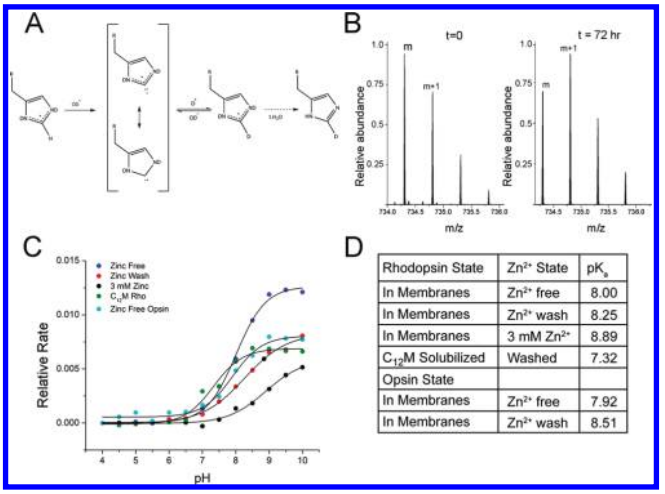

Rhodopsin State	Zn^{2+} State	pK_a
In Membranes	Zn^{2+} free	8.00
In Membranes	Zn^{2+} wash	8.25
In Membranes	3 mM Zn^{2+}	8.89
$C_{12}M$ Solubilized	Washed	7.32
Opsin State		
In Membranes	Zn^{2+} free	7.92
In Membranes	Zn^{2+} wash	8.51

FIGURE 2: Deuterium exchange on the C_2 hydrogen of His residues detected by mass spectroscopy depends on the pK_a of the residue. (A) HDX reaction scheme illustrating deuterium exchange at the C_2 position. (B) Peak intensities m + H and m + D of the His^{195} peptide (YTPHEETNNESF) at $t = 0$ and $t = 72$ h deuterium exchange at pH 8.0 reveal incorporation of deuterium at position C_2. The ratio of deuterated to nondeuterated ions depends on the His residue protonation state. (C) The midpoint of a sigmoidal curve fit to this data provides the His residue pK_a. (D) Zn^{2+} ion-dependent changes in the pK_a of His^{195}.

Table 1: Half-Lives of His-HDX for Membrane-Bound Rho and Opsin Indicate Differences in Their Membrane Environments[a]

His residue	rhodopsin half-life of HXD (h)	opsin half-life of HXD (h)
His^{65}	15.5 ± 1.9	9.1 ± 0.64
His^{100}	17.4 ± 5.7	32.1 ± 7.1
His^{152}	> 50	> 50
His^{195}	5.4 ± 0.15	21.8 ± 2.5
His^{211}	> 50	> 50
His^{278}	> 50	> 50

[a]All experiments were conducted in triplicate at pH 8.0 as described in detail in the Supporting Information.

exhibit any exchange as it is sequestered within the transmembrane domain and the exchange itself would be inhibited because of the proximity of the N_1 and N_2 atoms of the imidazole ring with either amino acid residues within this cluster or headgroups of phospholipids. These interactions could presumably impede the approach of bulk water molecules to the C_2 hydrogen, inhibiting the formation of the ylide needed for exchange of the C_2 hydrogen. The half-life of His-HDX was shorter for His^{100} and His^{195} in Rho than in opsin, whereas the exchange for cytoplasmic His^{65} (Figure 1A) indicated that it is more solvent-accessible in opsin (Table 1).

The fastest exchanging group in the experiments described above, His^{195}, also exhibited the largest differential in exchange rate between Rho and opsin, suggesting that this residue could be used to assess conformational changes in Rho in different states and environments. We found that its apparent pK_a was significantly affected by binding of Zn^{2+}, which was previously identified to be coordinated by this residue (*13*). As this His is also close to membranes and can interact with headgroups of phospholipids, we consistently found that its pK_a decreased when Rho was solubilized in dodecyl maltoside. pK_a values were found to have trends similar to but differed from those of Rho, suggesting that intracellular changes also occur in this intradiscal region as observed in recent NMR studies (*14*).

Significant differences are noted between the X-ray crystal structures of ground state Rho and its inactive end product, opsin (*15*). A second opsin structure that closely superposes with the first opsin structure features a bound peptide and was claimed by the authors to recapitulate the "active G-protein-binding state" (*4*). It must be noted that opsin activates G protein orders of magnitude more slowly than Meta II, the physiological active state of Rho, and furthermore, the true hallmark of any activated state of a GPCR should be its ability to catalyze nucleotide exchange on its cognate G protein. Transmission of the activating signal down the signaling cascade should be the gold standard for whether Rho or any GPCR has attained the activated state.

Using radiolytic footprinting in which $OH^{\bullet}$ radicals are generated with a millisecond pulse of synchrotron radiation, we showed that within the transmembrane region of Rho, residues in the proximity of crystallographically observed water molecules were preferentially labeled. Furthermore, we observed lower rates of modification in opsin as compared to that of either ground state Rho or photoactivated (Meta II) Rho. This is not surprising as fewer crystallographically observed waters are found in opsin than in Rho structures of similar resolution. With the His-HDX-MS technique, we extend these results to residues within the cytoplasmic and extracellular faces of the Rho protein. Surprisingly, rather than becoming more accessible to bulk solvent, His^{100} and His^{195} in

opsin exchanged with bulk solvent at rates decidedly slower than those of Rho.

While we cannot ascribe any of these changes in the half-life of deuterium exchange with solvent directly to inter-Rho contacts, examination of dimer interfaces observed in several crystal forms of Rho as well as other GPCR structures and oligomeric models of Rho appear to reveal reasons for some of the observed differences. While an explanation for the disparity in exchange rates observed for His^{195} exchange in opsin versus Rho remains elusive, an ionic interaction between His^{100} and Tyr^{96} observed in the 2I37 and 2I36 Rho crystal structures but not the 3CAP opsin structure may underlie these differences through stabilization of the cationic imidazolium of this residue, the concentration of which is directly proportional to the HDX rate (*16*). While His^{152} exchanges too slowly with bulk solvent for us even to determine a $t_{1/2}$, examination of oligomeric models of Rho suggests that interactions of His^{152} with His^{152} on an adjacent oligomer might negatively impact the solvent accessibility of this residue.

One consequence of dietary zinc deficiency is the development of severe retinal degeneration, presumably due to destabilization of Rho. Using single-molecule force microscopy, we previously demonstrated that Zn^{2+} provides a stabilizing influence upon Rho (*17*). This work was extended by employing His-HDX-MS as a readout for changes in Rho embedded in ROS membranes due to the presence or absence of Zn^{2+}. We found that, in addition to the aforementioned differential in the half-life of exchange for His^{195}, its apparent pK_a changed markedly in a Zn^{2+} concentration-dependent manner. Notably, this His residue, which had the fastest exchange rate of all His residues within Rho, is close to three carboxylate groups and also coordinates a Zn^{2+} ion in several Rho crystal structures. We postulate that the observed differences in the pK_a values of His^{195} are a direct manifestation of remodeling the Zn^{2+}-binding site adjacent to this residue. The shift to an even higher pK_a in the presence of 3 mM Zn^{2+} indicates that the electron donating effect by the neighboring environment to this imidazole ring increases upon Zn^{2+} binding. As there are high levels of Zn^{2+} in the CNS as well as the retina, it is possible that the Zn^{2+} performs a similar role, stabilizing other GPCRs as well.

In short, by taking advantage of intrinsic His residues found spaced throughout Rho, we monitored long time scale structural rearrangements previously inaccessible by other means. Results with Rho indicate that this methodology might prove useful in examining and/or monitoring structural rearrangements in native source proteins and other difficult-to-analyze proteins without modifying their intrinsic structures.

ACKNOWLEDGMENT

We thank Dr. L. T. Webster Jr. for valuable comments.

SUPPORTING INFORMATION AVAILABLE

Detailed information providing experimental procedures, calculation of deuterium exchange, and mass spectrometric analysis. This material is available free of charge via the Internet at http://pubs.acs.org.

REFERENCES

1. Palczewski, K. (2006) *Annu. Rev. Biochem. 75*, 743–767.
2. Park, P. S., Lodowski, D. T., and Palczewski, K. (2008) *Annu. Rev. Pharmacol. Toxicol. 48*, 107–141.
3. Salom, D., Lodowski, D. T., Stenkamp, R. E., Le Trong, I., Golczak, M., Jastrzebska, B., Harris, T., Ballesteros, J. A., and Palczewski, K. (2006) *Proc. Natl. Acad. Sci. U.S.A. 103*, 16123–16128.
4. Scheerer, P., Park, J. H., Hildebrand, P. W., Kim, Y. J., Krauss, N., Choe, H. W., Hofmann, K. P., and Ernst, O. P. (2008) *Nature 455*, 497–502.
5. Farrens, D. L., Altenbach, C., Yang, K., Hubbell, W. L., and Khorana, H. G. (1996) *Science 274*, 768–770.
6. Garczarek, F., and Gerwert, K. (2006) *Nature 439*, 109–112.
7. Angel, T. E., Gupta, S., Jastrzebska, B., Palczewski, K., and Chance, M. R. (2009) *Proc. Natl. Acad. Sci. U.S.A. 106*, 14367–14372.
8. Zhang, X., Chien, E. Y. T., Chalmers, M. J., Pascal, B. D., Gatchalian, J., Stevens, R. C., and Griffin, P. R. (2010) *Anal. Chem. 82*, 1100–1108.
9. Hebling, C. M., Morgan, C. R., Stafford, D. W., Jorgenson, J. W., Rand, K. D., and Engen, J. R. (2010) *Anal. Chem. 82*, 5415–5419.
10. Weitz, C. J., and Nathans, J. (1992) *Neuron 8*, 465–472.
11. Beck, M., Sakmar, T. P., and Siebert, F. (1998) *Biochemistry 37*, 7630–7639.
12. Miyagi, M., and Nakazawa, T. (2008) *Anal. Chem. 80*, 6481–6487.
13. Stojanovic, A., Stitham, J., and Hwa, J. (2004) *J. Biol. Chem. 279*, 35932–35941.
14. Ahuja, S., Hornak, V., Yan, E. C., Syrett, N., Goncalves, J. A., Hirshfeld, A., Ziliox, M., Sakmar, T. P., Sheves, M., Reeves, P. J., Smith, S. O., and Eilers, M. (2009) *Nat. Struct. Mol. Biol. 16*, 168–175.
15. Park, J. H., Scheerer, P., Hofmann, K. P., Choe, H. W., and Ernst, O. P. (2008) *Nature 454*, 183–187.
16. Vaughan, J., Mughrabi, Z. E., and Wu, C. (1970) *J. Org. Chem. 35*, 1141–1145.
17. Park, P. S., Sapra, K. T., Kolinski, M., Filipek, S., Palczewski, K., and Muller, D. J. (2007) *J. Biol. Chem. 282*, 11377–11385.